HHS Public Access

Author manuscript

Nat Cell Biol. Author manuscript; available in PMC 2014 February 01.

Published in final edited form as:

Nat Cell Biol. 2013 August ; 15(8): 926–936. doi:10.1038/ncb2796.

Apical domain polarization localizes actin-myosin activity to drive ratchet-like apical constriction

Frank M. Mason[1], **Michael Tworoger**[1], and **Adam C. Martin**[1]

[1]Department of Biology, Massachusetts Institute of Technology, Cambridge, MA 02142, USA

Abstract

Apical constriction promotes epithelia folding, which changes tissue architecture. During *Drosophila* gastrulation, mesoderm cells exhibit repeated contractile pulses that are stabilized such that cells apically constrict like a ratchet. The transcription factor Twist is required to stabilize cell shape, however it is unknown how Twist spatially coordinates downstream signals to prevent cell relaxation. We find that during constriction, Rho-associated kinase (Rok) is polarized to the middle of the apical domain (medioapical cortex), separate from adherens junctions (AJs). Rok recruits or stabilizes medioapical myosin II (Myo-II), which contracts dynamic medioapical actin cables. The formin Diaphanous mediates apical actin assembly to suppress medioapical E-Cadherin localization and form stable connections between the medioapical contractile network and AJs. Twist is not required for apical Rok recruitment, but instead polarizes Rok medioapically. Therefore, Twist establishes “radial” cell polarity of Rok/Myo-II and E-Cadherin and promotes medioapical actin assembly in mesoderm cells to stabilize cell shape fluctuations.

Introduction

Apical constriction is an epithelial cell shape change that promotes tissue bending during developmental processes such as gastrulation and neural tube closure[1–3]. Apical constriction bends epithelia by transforming columnar cells to a wedge shape[4]. During *Drosophila* gastrulation, the apical constriction of presumptive mesoderm cells along the ventral midline results in ventral furrow (VF) formation and tissue invagination[5,6]. Apical constriction and VF formation are induced by the expression of two transcription factors, Twist and Snail[5,7,8]. A major question in the field has been how Twist and Snail promote force generation and apical constriction at the molecular level.

Forces that drive apical constriction are generated by the contraction of an actin filament (F-actin) network by the molecular motor non-muscle myosin II (Myo-II)[9–12]. In VF cells, and

Corresponding author: Adam C. Martin, acmartin@mit.edu, 31 Ames St., Cambridge, MA 02142, USA.

Author Contributions

F.M.M. designed and performed experiments, analysed data and wrote the manuscript. M.T. designed and performed experiments. A.C.M. designed and performed experiments, analysed data, supervised the project and wrote the manuscript.

Competing financial interests

The authors declare no competing financial interests.

many other contractile systems, Myo-II contractions and cell shape changes occur in a pulsed or ratchet-like manner[13–24]. Contractile pulses in VF cells occur in the F-actin-Myo-II network spanning the apical domain (medioapical cortex), which pull peripheral adherens junctions (AJs) inward (Fig. 1a)[20]. After a contraction pulse, the constricted state of the cell is stabilized to incrementally decrease apical area, similar to the mechanism of a ratchet[20]. Twist and Snail regulate distinct steps of this ratchet-like constriction[20]. Snail is required to initiate contractile pulses, but the mechanism is unclear. Twist is required to stabilize cell shape between pulses. Two Twist transcriptional targets, Folded gastrulation (Fog) and T48, could function in parallel to activate the Rho1 GTPase apically (Fig. 1b)[25,26]. It is thought that apical secretion of Fog activates Rho1 signaling and Myo-II recruitment across the apical surface of VF cells[27–29]. How Rho1 stabilizes cell shape is not known and could depend on tension generated by medioapical or junctional cytoskeletal networks[13,22,30]. Therefore, elucidating the ratchet mechanism requires determining how Rho1 and its effectors regulate medioapical and junctional actin-myosin networks in response to Twist and Snail.

Contractile forces must be coupled to the AJs in order to generate cell and tissue shape changes[28,30–34]. AJ remodeling accompanies VF cell apical constriction, with subapical AJs being disassembled, which requires Snail, and spot junctions assembling at the apical cell-cell interfaces, which appears to require Twist (Fig. 1c)[26,28,30]. It is not known how signals that activate Myo-II are coordinated with AJ remodeling to couple contraction to AJs.

Here we visualize how the dynamics of the Myo-II, F-actin, and AJs are coordinated with the Rho1 GTPase pathway to dissect the mechanism of ratchet-like apical constriction.

Results

Ventral furrow cells exhibit radial cell polarity (RCP) of Rok/Myo-II and E-Cadherin

The Rho1 effector Rho-associated kinase (Rok) phosphorylates and activates Myo-II and is required for VF cell apical constriction, suggesting that apical Fog-dependent activation of Rok and Myo-II triggers apical constriction[28,35]. The importance of Rok in polarizing contraction is supported by the fact that planar polarized Rok localizes Myo-II contraction to anterior-posterior cell interfaces during convergent extension of the *Drosophila* germband cells[36–40]. Additionally, planar polarized Rok excludes Bazooka/Par-3 from the cortex, establishing complementary domains of Rok/MyoII and AJ proteins[40]. To test the role of Rok in VF cells, we examined Rok localization dynamics using either a kinase-dead Rok allele, Venus(or GFP)::Rok(K116A), or a Venus::Rok(WT) expressed in rok^2 mutant germline clones[40]. Venus(or GFP)::Rok(K116A) and Venus::Rok(WT) localization patterns were indistinguishable, and Venus::Rok(WT) rescued the VF invagination defect of rok^2 mutants[28], suggesting that both Venus::Rok alleles indicate the localization of endogenous Rok (Fig. 1d, e, f, and Supplemental Fig. 1). Rok exhibited apical accumulation in VF cells prior to Rok apical localization in the germband (Fig. 1d). Apical domain proteins normally localize directly above AJs or uniformly across the apical surface of epithelial cells[41,42]. However, Rok displayed an unexpected apical organization, initially exhibiting dispersed staining and then accumulating in medioapical foci as cells constricted (Fig. 1e, f, and Supplemental Fig. 1). In contrast to germband cells, where Rok is present at cell-cell

interfaces[40], Rok intensity appeared lowest at the junctions (Fig. 1f, g). Medioapical Rok foci colocalized with Myo-II, consistent with Rok recruiting or stabilizing Myo-II (Fig. 1h). Thus, similar to germband cells, Rok/Myo-II and E-Cadherin are enriched in different domains. However, in VF cells, Rok/Myo-II is concentrated in medioapical foci and AJs are present around the cell circumference, a pattern that we term “radial” cell polarity (RCP).

The Rho1 GTPase and its effectors exhibit distinct localization patterns

To determine if other Twist pathway components are polarized to medioapical foci, we examined the localization of Rho1 and a Rho1 effector that mediates unbranched actin polymerization and F-actin cable formation, the formin Diaphanous (Dia)[27,29,43]. Rho1 localized to medioapical foci that partially overlapped Rok foci, but also localized to the junctional domain (Fig. 2a). Dia partially colocalized with medioapical Rho1/Rok foci and junctional Rho1 (Fig. 2b, c). However, Dia exhibited more diffuse staining across the apical domain, which largely colocalized with the F-actin-Myo-II meshwork (Fig. 2d). Therefore, Rho1, Rok, and Dia are differentially localized in the apical domain of VF cells, which suggests that Twist and Rho1 spatially regulate F-actin and Myo-II activity during ratchet-like constriction.

Rok is required for medioapical F-actin network condensation

We hypothesized that the RCP of Rok might spatially control Myo-II activation or stabilization to regulate contractility or the organization of the apical F-actin network, both of which are important for apical constriction[44]. To determine how medioapical Rho1-Rok foci regulate F-actin network contraction in VF cells, we visualized F-actin and Myo-II dynamics by expressing the F-actin binding domain of Utrophin fused to GFP (Utr::GFP) and the regulatory light chain of Myo-II (*spaghetti squash*, *sqh* in *Drosophila*) fused to mCherry fluorescent protein (Myo::ChFP)[20,22]. Utr::GFP labels medioapical, junctional, and basolateral networks, similar to phalloidin staining in fixed embryos, demonstrating that Utr::GFP labels F-actin networks in an unbiased manner (Supplemental Fig. 2a, b). Similar to Rok localization, apical Myo-II recruitment occurs in VF cells before germband cells and was associated with structural changes in the F-actin network (Fig. 3a, and Supplemental Videos 1, 2). To analyze F-actin dynamics, we first used custom software to segment individual cells and quantify total apical F-actin levels during apical constriction[45]. In contrast to the increase in apical Myo-II intensity, we found that average total apical F-actin levels decrease over the course of apical constriction, suggesting that F-actin network depolymerization accompanies constriction (Supplemental Fig. 2c). However, during contraction pulses we often observed brief increases or stabilization of F-actin intensity (Fig. 3b, and Supplemental Fig. 2d, e). The increase or stabilization of F-actin intensity was associated with F-actin condensation into medioapical foci (Fig. 3c). Following F-actin condensation, F-actin foci were subsequently remodeled, often into cables, and F-actin intensity appeared to decrease as area stabilized (Fig. 3c, d, and Supplemental Fig. 2d). The mechanism for this F-actin remodeling is unclear, but F-actin depolymerization is possibly required to regenerate actin monomers that are then assembled into new F-actin cables. Medioapical F-actin condensation and dissolution occurred simultaneously with Myo-II (Fig. 3d–f), suggesting that F-actin condensation represents contraction of the medioapical F-actin cortex. To determine whether medioapical F-actin condensation requires Rok, we

injected embryos with the Rok inhibitor, Y-27632[46]. Y-27632-injected embryos failed to accumulate cortical Myo-II, consistent with previous observations[47], and cells did not constrict (Fig. 3g). However, medioapical F-actin was prominent in VF cells after Y-27632 injection. F-actin filaments or cables continuously assembled and disassembled (Fig. 3h, i, and Supplemental Video 3). F-actin cables originated from medioapically and junctionally, consistent with Rho1 and Dia localization at both locations (Fig. 3i). Despite robust medioapical F-actin assembly, F-actin cables failed to condense into medioapical foci in Y-27632 injected embryos (Supplemental Videos 2, 3). Thus, RCP of Rok is dispensable for medioapical F-actin assembly, but is required to condense medioapical F-actin cables that span the apical domain, presumably by targeting Myo-II to the medioapical cortex.

F-actin polymerization is required to couple medioapical contraction to cell-cell junctions

Our visualization of F-actin cable assembly at both the medioapical cortex and junctions of Y-27632-injected VF cells suggested that Rho1 could activate Dia to stimulate F-actin assembly across the apical domain. Furthermore, Y-27632-injected germband cells have less pronounced medioapical F-actin cables than in VF cells (Fig. 3h), supporting a previous study that suggested that signals in VF cells enhance medioapical F-actin assembly relative to germband cells[48]. To test the function of F-actin assembly during apical constriction, we injected embryos with Cytochalasin D (CytoD), which binds the barbed end of F-actin and inhibits polymerization[49]. High CytoD concentrations blocked apical constriction and disrupted the F-actin-Myo-II network, resulting in apical Myo-II spots that fail to coalesce, as previously reported (Fig. 4a, b)[20]. We titrated the amount of injected CytoD to identify processes that were most sensitive to reduced F-actin assembly. Lower CytoD concentrations allowed VF cells to assemble an apical F-actin-Myo-II network and initiate constriction (Fig. 4a, b). Normally, VF cells undergo contractile pulses, resulting in a significant positive cross-correlation between calculated constriction rate and Myo-II accumulation rate due to in-phase contraction pulses (Supplemental Fig. 2f)[20,30]. Despite undergoing apical constriction and Myo-II accumulation, we failed to observe obvious Myo-II pulses in embryos injected with low CytoD concentrations, which was supported by the lack of a cross-correlation between constriction rate and myosin rate (Fig. 4c, d). Also, low CytoD concentrations destabilized the connection between the medioapical actin-myosin network and cell-cell junctions, with networks transiently losing and then regaining connections to each other across the tissue (Fig. 4a, and Supplemental Videos 4–6). Low CytoD concentrations resulted in gaps in the medioapical F-actin cortex that preceded junction detachments, demonstrating that defects in medioapical F-actin network continuity precipitate separation of the medioapical network from cell-cell junctions (Fig. 4e, and Supplemental Video 7). Overall, these results demonstrate that robust apical F-actin assembly is critical for medioapical contraction pulses and to form a stable connection between the contractile medioapical domain and AJs.

Diaphanous couples the contractile network to junctions, possibly by polarizing AJ localization

Dia was previously shown to be important for VF formation[50]. To determine whether Dia mediates F-actin assembly and junction attachment, we generated germline clones using the partial loss-of-function *dia*^{5} allele (*dia*^{M})[50]. We were unable to analyze VF formation in

dia^{M} embryos with strong phenotypes, because these had severe defects during cellularization, which precedes gastrulation[51–53]. However, *dia*^{M} embryos with mild cellularization phenotypes had apical Myo-II accumulation and exhibited transient losses in the connections between medioapical F-actin-Myo-II network and junctions, similar to embryos injected with low CytoD concentrations (Fig. 5a, b, and Supplemental Video 8). Together with the CytoD injections, our results suggest that Dia-dependent F-actin assembly in part mediates medioapical and junctional F-actin assembly to link the medioapical cortex to AJs.

Dia-mediated F-actin assembly could facilitate apical constriction by generating medioapical F-actin cables to facilitate Myo-II contraction (Fig. 3c and 4e), but could also regulate the organization of AJs[39,50,54,55]. Because Twist has been proposed to be required for apical AJ formation[26], we examined E-Cadherin localization in *dia*^{M} mutants. We found that E-Cadherin localized apically in *dia*^{M} mutants. However, E-Cadherin was not restricted to the junctional domain, but spread across the entire apical surface, which is different from E-Cadherin localization in *dia*^{M} mutants for other cell types[50] (Fig. 5c). While it is possible that some of this apical E-Cadherin is present in endocytic vesicles and not cortical (Supplemental Fig. 3)[50,56], it is clear that there is a disruption in the localization and polarity of E-Cadherin in *dia*^{M} mutants. E-Cadherin polarity was also lost after CytoD injection (Fig. 5d). Interestingly, defects in Dia-mediated F-actin assembly results in a similar loss of cortical domains or “compartments” during the process of cellularization, potentially from misregulation of endocytic activity[53,57,58]. Thus, Dia-mediated F-actin assembly is required in VF cells for the RCP of apical E-Cadherin, restricting E-Cadherin to the junctional domain. The cell-cell attachment defect is unlikely to result from lower E-Cadherin levels at the junctional domain because medioapical networks can regain attachments (Fig. 5a), whereas AJ mutants result in permanent dissociations between the medioapical network and the junctions[30]. We propose that Dia-mediated F-actin assembly could facilitate the attachment between the medioapical contractile network and junctions by spatially segregating contractile and junctional components into distinct domains, providing definitive anchor points at the cell periphery (Fig. 5e, AJ depolarization). In addition, Dia could be required to assemble medioapical and junctional F-actin cables to link the two domains (Fig. 5e, Network dissolution).

Twist is required for a continuous medioapical F-actin meshwork

Our results demonstrate that the spatial regulation of Myo-II recruitment, F-actin assembly, and AJ organization cooperate to achieve ratchet-like apical constriction. Thus, Twist expression could stabilize pulsed contractions by controlling F-actin, Myo-II, or AJs in specific cellular domains. Recently, cell shape fluctuations resulting from medioapical contractions were proposed to be stabilized by junctional actin-myosin networks[13,22]. Because Rho1 and Dia localize both medioapically and junctionally in VF cells, we tested whether Twist is required for either of these F-actin networks. In contrast to wild-type VF cells, which exhibit a continuous meshwork of medioapical and junctional F-actin cables, visualization of Utr::GFP in *twist* mutants demonstrated that the *twist* mutant results in dynamic medioapical F-actin puncta that fail to form cables across the apical domain (Fig. 6a, and Supplemental Video 9). Importantly, *twist* mutants have junctional F-actin cables

(Fig. 6a, b), which display similar intensity to junctional F-actin in lateral germband cells (furrow:germband ratio=0.96, n=20 cells). *twist* mutants exhibited a lower medioapical:junctional F-actin ratio, suggesting that *twist* mutants are defective in the formation of the medioapical F-actin network relative to junctional F-actin (Fig. 6c). This contrasts with *snail* mutants, which lack medioapical and apical junctional F-actin cables (Fig. 6a–c, and Supplemental Video 9). Because Twist is required for cell shape stabilization after pulses, we examined F-actin dynamics over the course of individual pulsatile events. In wild-type cells, F-actin levels usually increase or remain stable during the contraction and persist as F-actin cables (Fig. 3b). However, in *twist* mutants, the F-actin network is always punctate and F-actin levels decrease during contraction (Fig. 6a, d, e). Overall, these results suggest that Twist facilitates medioapical F-actin assembly. Importantly, *twist* mutants did not result in E-Cadherin depolarization, suggesting that the medioapical meshwork of F-actin cables contributes to cell shape stabilization independently from regulating E-Cadherin RCP (Fig. 7e).

twist mutants result in the inversion of Rok and Myo-II RCP

We previously demonstrated that *twist* is required for apical Myo-II persistence following pulsed contractions[30]. The RCP of Rok suggests that medioapical Myo-II phosphorylation could be coordinated with F-actin assembly to stabilize medioapical actin-myosin cables that prevent cell relaxation. Therefore, we examined whether Twist regulates the RCP of Rok. Previous work suggested that the Twist pathway is required for the apical localization of the Rho1 activator, DRhoGEF2 (Fig. 1b)[26]. Unexpectedly, we found apical Rok enrichment in *twist* mutants VF cells (Supplemental Fig. 4). However, the normal RCP of Rok was inverted in *twist* mutants, with Rok exhibiting junctional localization at three-way vertices, rather than localizing medioapically (Fig. 7a). *snail* mutants also exhibited a defect in medioapical Rok recruitment (Fig. 7a). However, Rok localizes to a subapical position, consistent with the position of AJs in *snail* mutants (Fig. 7b)[26]. Subapical Rok localization did not exhibit a clear dorsal-ventral polarity in *snail* mutants, demonstrating that Twist requires Snail to recruit apical Rok (Supplemental Fig. 4). Consistent with Rok locally stabilizing Myo-II, changes in Myo-II localization mirrored Rok, with Myo-II becoming enriched in apical or subapical vertices in *twist* and *snail* mutants, respectively (Fig. 7c, d). In *twist* and *snail* mutants, Myo-II, and presumably Rok, colocalized with apical and subapical AJs, respectively (Fig. 7e). Thus, Twist and Snail are required to polarize Rok to the medioapical domain and away from AJs. *twist* mutants continued to exhibit transient medioapical Myo-II pulses between Myo-II foci at vertices, but medioapical Myo-II was not stabilized (Fig. 7c). Thus, medioapical Rok foci appear to stabilize Myo-II in the medioapical cortex of VF cells. We propose that the function of Twist is not simply to activate apical Rho1 and Rok, but that Twist polarizes Rho1 signaling in the plane of the apical surface, leading to the polarization of Rok and Myo-II to the medioapical domain.

Discussion

We have demonstrated a spatial organization to Twist pathway components, which polarizes Rok/Myo-II and E-Cadherin/AJs to medioapical and junctional domains, respectively. The enrichment of Rok/Myo-II and E-Cadherin/AJs to separate domains is similar to the process

of cell-cell intercalation during *Drosophila* germband extension[36–40]. However, Rok/Myo-II and AJ components exhibit planar cell polarity (PCP) in germband cells, whereas they exhibit "radial" cell polarity (RCP) in VF cells (Fig. 8a). Dia-mediated F-actin polymerization appears to maintain E-Cadherin polarity and link the medioapical and junctional domains in VF cells, allowing contractile forces to be stably transmitted across AJs. Thus, Myo-II stabilization, AJ organization, and F-actin assembly are temporally and spatially coordinated to drive ratchet-like apical constriction (Fig. 8b).

During VF cell apical constriction, Rok becomes concentrated as medioapical foci and is absent or present at low levels at AJs. The RCP of Rok appears to target Myo-II accumulation to the medioapical domain. The importance of Rok localization is strongly supported by the fact that the RCP of both Rok and Myo-II are inverted in *twist* and *snail* mutants, with Rok and Myo-II accumulating inappropriately at AJs. Although Rok is improperly localized in both mutants, *twist* mutants still exhibit contractile pulses, suggesting that the apical Rok at AJs or low levels of Rok in the medioapical domain are sufficient to promote Myo-II pulses. We propose that Rok's localization increases Myo-II phosphorylation when Myo-II reaches the medioapical domain either by diffusion or contractile flow, leading to increased minifilament assembly and stabilization of Myo-II structures (Fig. 8b)[59,60]. The inappropriate localization of Rok in *twist* mutants suggests that Myo-II assembly in the medioapical domain, rather than junctions, is critical to stabilize cell shape between pulses for cells to constrict like a ratchet.

Medioapical contractility and epithelial tension requires that the contractile cortex be coupled to the junctional domain[30,33]. Rho1 and Dia localize to both the medioapical and junctional domains, and we observe F-actin cables originating from both locations in the absence of Rok and Myo-II activity. Reducing F-actin assembly using CytoD or dia^{M} mutants destabilizes the connection between the medioapical contractile network and the junctional domain. Interestingly, CytoD and dia^{M} mutants cause E-Cadherin to accumulate across the entire apical surface rather than being restricted to the junctional domain. Dia-mediated F-actin assembly could polarize E-Cadherin through clathrin-mediated endocytosis, as was described in germband cells[39], thus removing medioapical E-Cadherin. F-actin-dependent regulation of endocytosis has also been proposed to establish cortical domains during *Drosophila* cellularization[53,57,58]. Thus, Dia could function to separate E-Cadherin from peak Rok activity, creating discrete anchor points at cell-cell interfaces that can be pulled inwards by Myo-II. In addition, F-actin assembly is required to form a continuous meshwork of F-actin cables that connects the medioapical and junctional domains. *twist* mutants maintain E-Cadherin RCP but lack a continuous meshwork of medioapical F-actin cables, suggesting that F-actin assembly contributes to the actin-myosin ratchet independently from regulating AJ polarity.

Our data suggests that Myo-II localization and F-actin assembly are coordinated to prevent cell relaxation. First, disruption of F-actin turnover and meshwork formation using F-actin inhibitors, such as CytoD, does not disrupt apical Myo-II recruitment[20]. Second, F-actin cable assembly occurs continuously in Rok inhibitor injected embryos that lack apical Myo-II. Therefore, we propose that the combination of localizing Myo-II stabilization to the medioapical cortex while more broadly activating medioapical and junctional F-actin

assembly results in the formation of contractile cables that span the apical domain of VF cells and become anchored at discrete AJ sites (Fig. 8b). These actin-myosin cables could function like stress-fibers to prevent cell relaxation after contractile pulses and form a supracellular meshwork[30].

Planar polarized actomyosin and AJ localization results in cell-cell intercalation whereas radially polarized actomyosin and AJ localization causes apical constriction (Fig. 8a)[36,37,40,48]. This is illustrated by the fact that Rok and Dia localize medioapically in VF cells to drive apical constriction, whereas Dia activation in the germband induces Myo-II accumulation at vertical junctions that contain Rok[48]. Therefore, developmental cues, such as Twist and Snail, must properly orient Myo-II, F-actin assembly, and AJ organization to elicit the appropriate cell shape change[48]. Importantly, we show that the function of Twist is not simply to activate, but to polarize apical signals like Rok to spatially regulate Myo-II stabilization and F-actin assembly. Determining the mechanism that establishes RCP will be critical to determine how the common set of signaling and cytoskeletal proteins are regulated to generate different cell shape changes during morphogenesis[61,62].

Supplementary Material

Refer to Web version on PubMed Central for supplementary material.

Acknowledgments

We thank Jennifer Zallen, Sérgio Simões, Rodrigo Fernandez-Gonzalez, Thomas Lecuit, Mark Peifer, Steven Wasserman, and the Bloomington Stock Center for providing fly stocks or antibodies used in this study. In addition, we thank members of the Martin lab and A. Sokac, V. Hatini, T. Orr-Weaver for their comments on versions of this manuscript. This work was supported by grant R00GM089826 to A.C.M. from the National Institute of General Medical Sciences. Adam C. Martin is a Thomas D. and Virginia W. Cabot Career Development Assistant Professor of Biology.

References

1. Leptin M. Gastrulation movements: the logic and the nuts and bolts. Dev Cell. 2005; 8:305–320. [PubMed: 15737927]
2. Martin AC. Pulsation and stabilization: contractile forces that underlie morphogenesis. Developmental Biology. 2010; 341:114–125.10.1016/j.ydbio.2009.10.031 [PubMed: 19874815]
3. Sawyer JM, et al. Apical constriction: A cell shape change that can drive morphogenesis. Dev Biol. 2009:1–15.10.1016/j.ydbio.2009.09.009
4. Odell GM, Oster G, Alberch P, Burnside B. The mechanical basis of morphogenesis. I. Epithelial folding and invagination. Dev Biol. 1981; 85:446–462. [PubMed: 7196351]
5. Leptin M, Grunewald B. Cell shape changes during gastrulation in Drosophila. Development. 1990; 110:73–84. [PubMed: 2081472]
6. Sweeton D, Parks S, Costa M, Wieschaus E. Gastrulation in Drosophila: the formation of the ventral furrow and posterior midgut invaginations. Development. 1991; 112:775–789. [PubMed: 1935689]
7. Leptin M. twist and snail as positive and negative regulators during Drosophila mesoderm development. Genes Dev. 1991; 5:1568–1576. [PubMed: 1884999]
8. Nusslein-Volhard C, Wieschaus E, Kluding H. Mutations affecting the pattern of the larval cuticle in Drosophila melanogaster: I. Zygotic loci on the second chromosome. Roux's Archives of Developmental Biology. 1984; 193:267–282.
9. Hildebrand JD. Shroom regulates epithelial cell shape via the apical positioning of an actomyosin network. J Cell Sci. 2005; 118:5191–5203. [PubMed: 16249236]

10. Kasza KE, Zallen JA. Dynamics and regulation of contractile actin-myosin networks in morphogenesis. Current opinion in cell biology. 2011; 23:30–38.10.1016/j.ceb.2010.10.014 [PubMed: 21130639]
11. Lecuit T, Lenne PF, Munro E. Force generation, transmission, and integration during cell and tissue morphogenesis. Annual review of cell and developmental biology. 2011; 27:157–184.10.1146/annurev-cellbio-100109-104027
12. Young PE, Pesacreta TC, Kiehart DP. Dynamic changes in the distribution of cytoplasmic myosin during Drosophila embryogenesis. Development. 1991; 111:1–14. [PubMed: 1901784]
13. Blanchard GB, Murugesu S, Adams RJ, Martinez-Arias A, Gorfinkiel N. Cytoskeletal dynamics and supracellular organisation of cell shape fluctuations during dorsal closure. Development. 2010; 137:2743–2752.10.1242/dev.045872 [PubMed: 20663818]
14. Burnette DT, et al. A role for actin arcs in the leading-edge advance of migrating cells. Nature cell biology. 2011; 13:371–381.10.1038/ncb2205 [PubMed: 21423177]
15. David DJ, Tishkina A, Harris TJ. The PAR complex regulates pulsed actomyosin contractions during amnioserosa apical constriction in Drosophila. Development. 2010; 137:1645–1655.10.1242/dev.044107 [PubMed: 20392741]
16. Fernandez-Gonzalez R, Zallen JA. Oscillatory behaviors and hierarchical assembly of contractile structures in intercalating cells. Physical biology. 2011; 8:045005.10.1088/1478-3975/8/4/045005 [PubMed: 21750365]
17. Giannone G, et al. Periodic lamellipodial contractions correlate with rearward actin waves. Cell. 2004; 116:431–443. [PubMed: 15016377]
18. He L, Wang X, Tang HL, Montell DJ. Tissue elongation requires oscillating contractions of a basal actomyosin network. Nature cell biology. 2010; 12:1133–1142.10.1038/ncb2124 [PubMed: 21102441]
19. Kim HY, Davidson LA. Punctuated actin contractions during convergent extension and their permissive regulation by the non-canonical Wnt-signaling pathway. Journal of Cell Science. 2011; 124:635–646.10.1242/jcs.067579 [PubMed: 21266466]
20. Martin AC, Kaschube M, Wieschaus EF. Pulsed contractions of an actin-myosin network drive apical constriction. Nature. 2009; 457:495–499. [PubMed: 19029882]
21. Munro E, Nance J, Priess JR. Cortical flows powered by asymmetrical contraction transport PAR proteins to establish and maintain anterior-posterior polarity in the early C. elegans embryo. Dev Cell. 2004; 7:413–424. [PubMed: 15363415]
22. Rauzi M, Lenne PF, Lecuit T. Planar polarized actomyosin contractile flows control epithelial junction remodelling. Nature. 2010; 468:1110–1114.10.1038/nature09566 [PubMed: 21068726]
23. Sawyer JK, et al. A contractile actomyosin network linked to adherens junctions by Canoe/afadin helps drive convergent extension. Molecular biology of the cell. 2011; 22:2491–2508.10.1091/mbc.E11-05-0411 [PubMed: 21613546]
24. Solon J, Kaya-Copur A, Colombelli J, Brunner D. Pulsed forces timed by a ratchet-like mechanism drive directed tissue movement during dorsal closure. Cell. 2009; 137:1331–1342. [PubMed: 19563762]
25. Costa M, Wilson ET, Wieschaus E. A putative cell signal encoded by the folded gastrulation gene coordinates cell shape changes during Drosophila gastrulation. Cell. 1994; 76:1075–1089. [PubMed: 8137424]
26. Kölsch V, Seher T, Fernandez-Ballester GJ, Serrano L, Leptin M. Control of Drosophila gastrulation by apical localization of adherens junctions and RhoGEF2. Science. 2007; 315:384–386.10.1126/science.1134833 [PubMed: 17234948]
27. Barrett K, Leptin M, Settleman J. The Rho GTPase and a putative RhoGEF mediate a signaling pathway for the cell shape changes in Drosophila gastrulation. Cell. 1997; 91:905–915. [PubMed: 9428514]
28. Dawes-Hoang RE, et al. folded gastrulation, cell shape change and the control of myosin localization. Development. 2005; 132:4165–4178. [PubMed: 16123312]
29. Hacker U, Perrimon N. DRhoGEF2 encodes a member of the Dbl family of oncogenes and controls cell shape changes during gastrulation in Drosophila. Genes Dev. 1998; 12:274–284. [PubMed: 9436986]

30. Martin AC, Gelbart M, Fernandez-Gonzalez R, Kaschube M, Wieschaus EF. Integration of contractile forces during tissue invagination. The Journal of Cell Biology. 2010; 188:735–749.10.1083/jcb.200910099 [PubMed: 20194639]
31. Cox RT, Kirkpatrick C, Peifer M. Armadillo is required for adherens junction assembly, cell polarity, and morphogenesis during Drosophila embryogenesis. The Journal of Cell Biology. 1996; 134:133–148. [PubMed: 8698810]
32. Gorfinkiel N, Arias AM. Requirements for adherens junction components in the interaction between epithelial tissues during dorsal closure in Drosophila. J Cell Sci. 2007; 120:3289–3298. [PubMed: 17878238]
33. Roh-Johnson M, et al. Triggering a cell shape change by exploiting preexisting actomyosin contractions. Science. 2012; 335:1232–1235.10.1126/science.1217869 [PubMed: 22323741]
34. Sawyer JK, Harris NJ, Slep KC, Gaul U, Peifer M. The Drosophila afadin homologue Canoe regulates linkage of the actin cytoskeleton to adherens junctions during apical constriction. J Cell Biol. 2009; 186:57–73. [PubMed: 19596848]
35. Bresnick AR. Molecular mechanisms of nonmuscle myosin-II regulation. Curr Opin Cell Biol. 1999; 11:26–33. [PubMed: 10047526]
36. Bertet C, Sulak L, Lecuit T. Myosin-dependent junction remodelling controls planar cell intercalation and axis elongation. Nature. 2004; 429:667–671.10.1038/nature02590 [PubMed: 15190355]
37. Blankenship JT, Backovic ST, Sanny JS, Weitz O, Zallen JA. Multicellular rosette formation links planar cell polarity to tissue morphogenesis. Dev Cell. 2006; 11:459–470.10.1016/j.devcel.2006.09.007 [PubMed: 17011486]
38. Fernandez-Gonzalez R, de Simoes SM, Roper JC, Eaton S, Zallen JA. Myosin II dynamics are regulated by tension in intercalating cells. Developmental cell. 2009; 17:736–743.10.1016/j.devcel.2009.09.003 [PubMed: 19879198]
39. Levayer R, Pelissier-Monier A, Lecuit T. Spatial regulation of Dia and Myosin-II by RhoGEF2 controls initiation of E-cadherin endocytosis during epithelial morphogenesis. Nature cell biology. 2011; 13:529–540.10.1038/ncb2224 [PubMed: 21516109]
40. de Simoes SM, et al. Rho-kinase directs Bazooka/Par-3 planar polarity during Drosophila axis elongation. Developmental cell. 2010; 19:377–388.10.1016/j.devcel.2010.08.011 [PubMed: 20833361]
41. Fletcher GC, Lucas EP, Brain R, Tournier A, Thompson BJ. Positive feedback and mutual antagonism combine to polarize Crumbs in the Drosophila follicle cell epithelium. Current biology : CB. 2012; 22:1116–1122.10.1016/j.cub.2012.04.020 [PubMed: 22658591]
42. Harris TJ, Peifer M. The positioning and segregation of apical cues during epithelial polarity establishment in Drosophila. The Journal of Cell Biology. 2005; 170:813–823.10.1083/jcb.200505127 [PubMed: 16129788]
43. Goode BL, Eck MJ. Mechanism and function of formins in the control of actin assembly. Annu Rev Biochem. 2007; 76:593–627.10.1146/annurev.biochem.75.103004.142647 [PubMed: 17373907]
44. Fox DT, Peifer M. Abelson kinase (Abl) and RhoGEF2 regulate actin organization during cell constriction in Drosophila. Development. 2007; 134:567–578. [PubMed: 17202187]
45. Gelbart MA, et al. Volume conservation principle involved in cell lengthening and nucleus movement during tissue morphogenesis. Proceedings of the National Academy of Sciences of the United States of America. 2012; 109:19298–19303.10.1073/pnas.1205258109 [PubMed: 23134725]
46. Uehata M, et al. Calcium sensitization of smooth muscle mediated by a Rho-associated protein kinase in hypertension. Nature. 1997; 389:990–994.10.1038/40187 [PubMed: 9353125]
47. Royou A. Cortical recruitment of nonmuscle myosin II in early syncytial Drosophila embryos: its role in nuclear axial expansion and its regulation by Cdc2 activity. The Journal of Cell Biology. 2002; 158:127–137.10.1083/jcb.200203148 [PubMed: 12105185]
48. Bertet C, Rauzi M, Lecuit T. Repression of Wasp by JAK/STAT signalling inhibits medial actomyosin network assembly and apical cell constriction in intercalating epithelial cells. Development. 2009; 136:4199–4212.10.1242/dev.040402 [PubMed: 19934015]

49. Cooper JA. Effects of cytochalasin and phalloidin on actin. The Journal of Cell Biology. 1987; 105:1473–1478. [PubMed: 3312229]
50. Homem CC, Peifer M. Diaphanous regulates myosin and adherens junctions to control cell contractility and protrusive behavior during morphogenesis. Development. 2008; 135:1005–1018. [PubMed: 18256194]
51. Afshar K, Stuart B, Wasserman SA. Functional analysis of the Drosophila diaphanous FH protein in early embryonic development. Development. 2000; 127:1887–1897. [PubMed: 10751177]
52. Grosshans J, et al. RhoGEF2 and the formin Dia control the formation of the furrow canal by directed actin assembly during Drosophila cellularisation. Development. 2005; 132:1009–1020. [PubMed: 15689371]
53. Yan S, et al. The F-BAR protein Cip4/Toca-1 antagonizes the formin Diaphanous in membrane stabilization and compartmentalization. Journal of Cell Science. 201310.1242/jcs.118422
54. Carramusa L, Ballestrem C, Zilberman Y, Bershadsky AD. Mammalian diaphanous-related formin Dia1 controls the organization of E-cadherin-mediated cell-cell junctions. Journal of Cell Science. 2007; 120:3870–3882.10.1242/jcs.014365 [PubMed: 17940061]
55. Sahai E, Marshall CJ. ROCK and Dia have opposing effects on adherens junctions downstream of Rho. Nature cell biology. 2002; 4:408–415.10.1038/ncb796 [PubMed: 11992112]
56. Roeth JF, Sawyer JK, Wilner DA, Peifer M. Rab11 helps maintain apical crumbs and adherens junctions in the Drosophila embryonic ectoderm. PLoS One. 2009; 4:e7634.10.1371/journal.pone.0007634 [PubMed: 19862327]
57. Sokac AM, Wieschaus E. Zygotically controlled F-actin establishes cortical compartments to stabilize furrows during Drosophila cellularization. Journal of Cell Science. 2008; 121:1815–1824.10.1242/jcs.025171 [PubMed: 18460582]
58. Sokac AM, Wieschaus E. Local actin-dependent endocytosis is zygotically controlled to initiate Drosophila cellularization. Dev Cell. 2008; 14:775–786. [PubMed: 18477459]
59. Watanabe T, Hosoya H, Yonemura S. Regulation of myosin II dynamics by phosphorylation and dephosphorylation of its light chain in epithelial cells. Molecular biology of the cell. 2007; 18:605–616.10.1091/mbc.E06-07-0590 [PubMed: 17151359]
60. Uehara R, et al. Determinants of myosin II cortical localization during cytokinesis. Current biology : CB. 2010; 20:1080–1085.10.1016/j.cub.2010.04.058 [PubMed: 20541410]
61. Mason FM, Martin AC. Tuning cell shape change with contractile ratchets. Current opinion in genetics & development. 2011; 21:671–679.10.1016/j.gde.2011.08.002 [PubMed: 21893409]
62. Montell DJ. Morphogenetic cell movements: diversity from modular mechanical properties. Science. 2008; 322:1502–1505. [PubMed: 19056976]

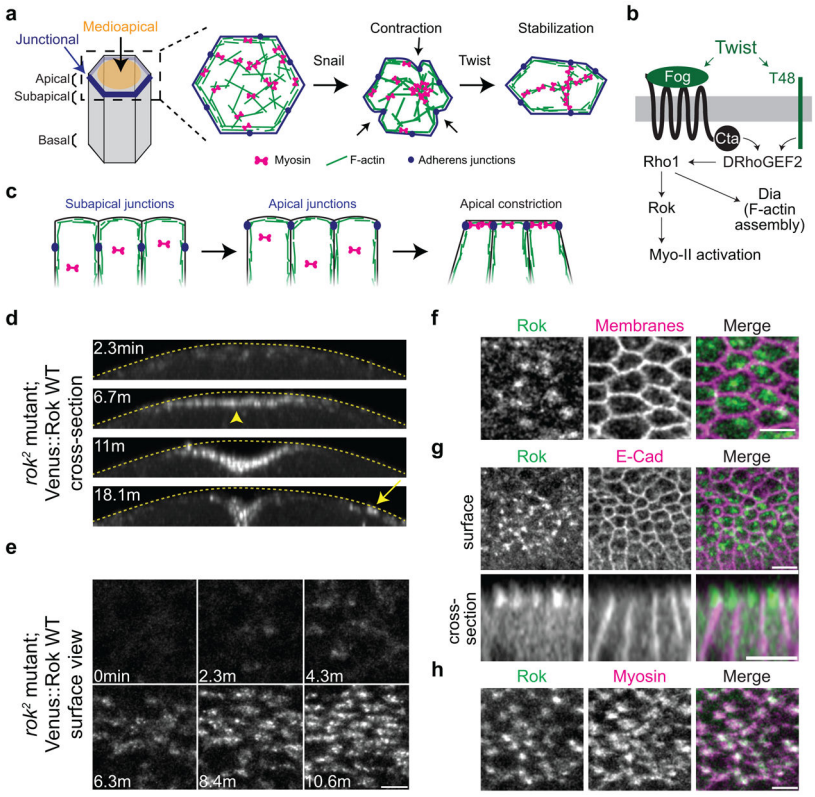

Figure 1.

Rok and E-Cadherin exhibit “radial” cell polarity (RCP) in ventral furrow cells.

(a) Diagram of ventral furrow cell and model of apical constriction. Snail is required to initiate contraction, and Twist stabilizes the contracted cell shape. During the stabilization, F-actin and Myo-II are often remodeled from foci into fibers. **(b)** Schematic of the Twist pathway. Twist activates the expression of Fog and T48, leading to Rho1 activation, which is proposed to activate Myo-II via Rok and stimulate F-actin assembly through Dia. **(c)** Model of AJ remodeling in ventral furrow cells. AJ initially assemble subapically then move apically into spot junctions when contraction initiates. **(d)** Rok is apically enriched in ventral furrow cells (arrowhead) prior to more lateral germband cells (arrow). Images are projections of cross-sections from a time-lapse movie of a *rok*^{2} germline mutant embryo expressing Venus::Rok(WT). Dotted yellow line marks the vitelline membrane. **(e)** Rok localizes to medioapical foci and patches. Surface view of same embryo in **d. (f)** Rok is polarized to a medioapical focus in individual cells. Images are from live embryo expressing Venus::Rok(K116A) (apical surface projection) and Gap43::ChFP (plasma membranes, subapical section). **(g)** Rok localizes to the medioapical surface between AJs. Images are from fixed embryo expressing GFP::Rok(K116A) (apical projection) and stained for E-Cadherin (subapical section). Images are surface view (top) and cross-sections (bottom). **(h)** Rok colocalizes with apical Myo-II. Images are from live embryo expressing Myo::ChFP and GFP::Rok(K116A). Scale bars are 5μm.

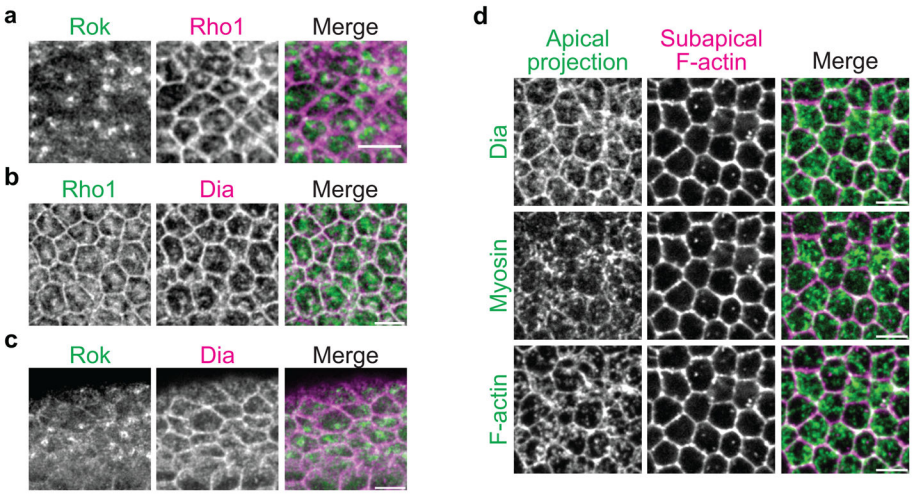

Figure 2.

Rho1 pathway components exhibit distinct localizations across the apical surface. **(a)** Rho1 localizes to medioapical foci and the junctional domain. Apical surface projection of a fixed embryo expressing GFP::Rok(K116A) and stained for Rho1. **(b)** Diaphanous (Dia) colocalizes with Rho1 in both the medioapical and junctional domains. Images are apical surface projections from a fixed embryo expressing GFP::Rho1 and stained for Dia. **(c)** Colocalization of Rok and Dia. Images are apical surface projections from a fixed embryo expressing GFP::Rok(K116A) and stained for Dia. **(d)** Dia localizes to the medioapical F-actin and Myo-II meshwork. Images are apical surface projections from the same fixed Myo::GFP embryo stained for Dia and F-actin (phalloidin). All scale bars are 5μm.

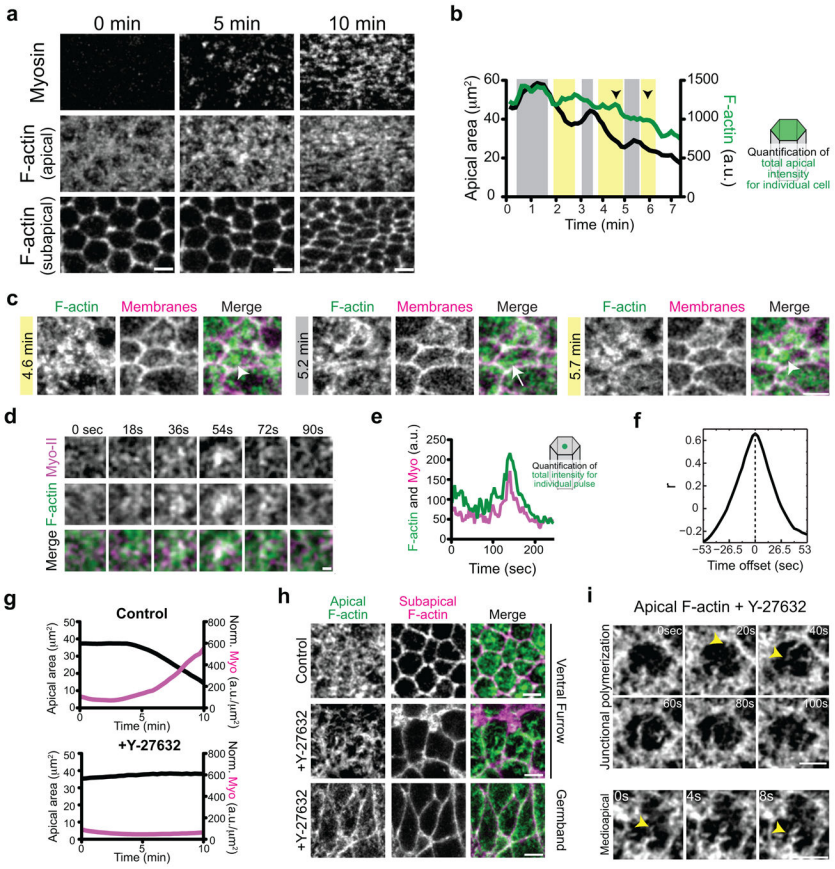

Figure 3.

Polarized Rok and Myo-II condenses dynamic medioapical F-actin cables.

(a) F-actin meshwork organization during ventral furrow formation. Time-lapse images are from live embryos expressing Myo::ChFP (Myosin) and Utr::GFP (F-actin). Apical Myo-II and F-actin are apical z-projections and sub-apical F-actin is one subapical section. Scale bar is 5μm. **(b)** F-actin levels slightly increase or remain stable during contraction pulses. Quantification of total apical F-actin levels (green) and area (black) in an individual cell from a live embryo expressing Utr::GFP and Gap43::ChFP. Contractile pulses are highlighted (yellow) and the arrowheads indicate a slight increase in F-actin intensity that corresponds to F-actin condensation in **c. (c)** F-actin is dynamically remodeled during and after contraction pulses. Time-lapse images represent different phases of the contraction cycle. Contractile pulses and increases in F-actin levels (yellow highlights) are associated with the condensation of medioapical F-actin into foci (arrowheads). During stabilization phases (grey), F-actin foci are remodeled, often into cables (arrow). Images of cell and arrowheads corresponds to pulses in **b**. Scale bar is 5μm. **(d)** F-actin condensation occurs with Myo-II accumulation. Time-lapse images are from live embryo expressing Myo::ChFP and Utr::GFP. Scale bar is 3μm. **(e)** Graph of a representative contraction pulse demonstrates that total F-actin and Myo-II intensities within a subcellular region increase and decrease at the same time. **(f)** Myo-II and F-actin coalesce simultaneously. Graph of mean time-resolved cross-correlation analysis of F-actin and Myo-II intensities within pulses (n=25 pulses) demonstrates that correlation peaks at zero seconds. **(g)** Rok is required for Myo-II

accumulation and apical constriction. Curves represent average apical area (black) and apical Myo-II intensity (magenta) in control (n=77 cells) and Y-27632 injected (n=82 cells) embryos. **(h)** Condensation of medioapical F-actin cables requires Rok activity. Representative images from embryos expressing Utr::GFP and injected with solvent (control) or Y-27632 (Rok inhibitor). Note the presence of F-actin cables in Y-27632 injected ventral furrow cells, which are not prominent in germband cells. Scale bar is 5μm. **(i)** Rok is not required for medioapical F-actin assembly. Representative time-lapse images are from a Utr::GFP expressing embryo that is injected with Y-27632. Arrowheads indicate F-actin cable appearance and elongation. Scale bar is 5μm.

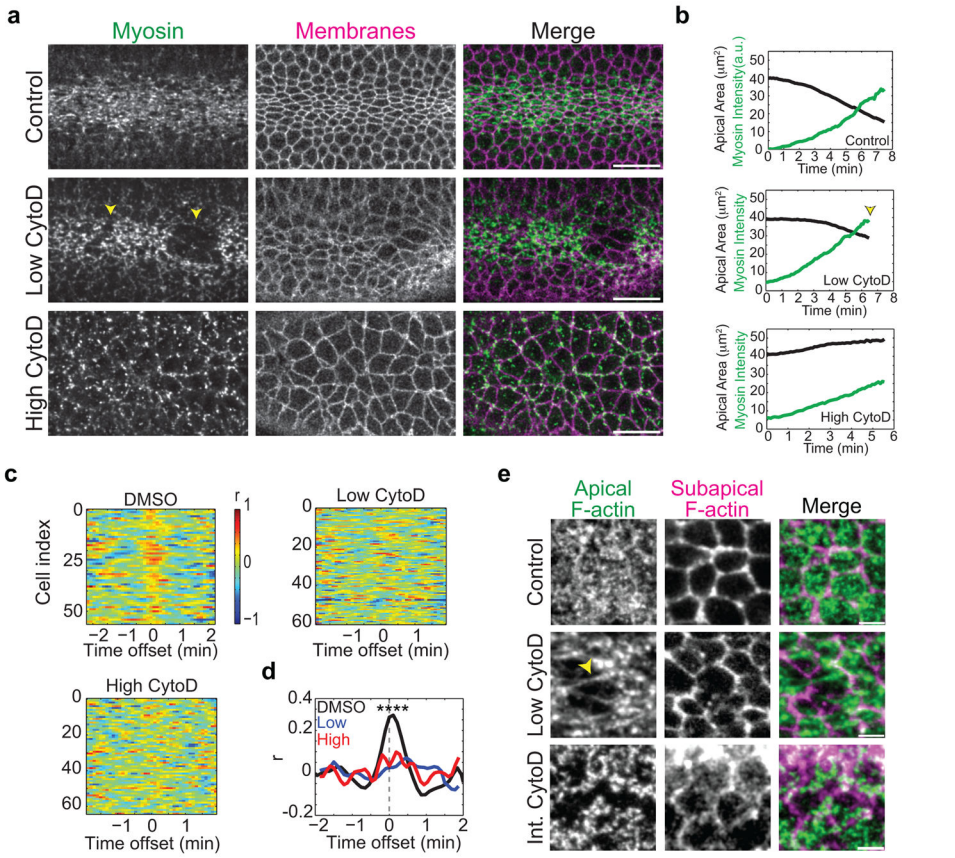

Figure 4.

F-actin polymerization is required to couple the contractile network to the junctions. **(a)** Titration of actin dynamics with CytoD identifies distinct functions for F-actin polymerization. Images are from live embryos expressing Myo::GFP and Gap43::ChFP. Embryos were injected with solvent (control), 0.125 mg/mL CytoD (low CytoD), or 5 mg/mL CytoD (high CytoD). Note low CytoD destabilizes the connection between the medioapical Myo-II network and cell-cell junctions, leading to tears in the supracellular Myo-II network (arrowheads). Cellular and tissue-wide Myo-II networks are disrupted with high CytoD. Scale bars are 20μm. **(b)** Mean apical area and Myo-II intensity for different CytoD doses. Data are from representative embryos injected with solvent (control, n=56 cells), low CytoD (n=86 cells), and high CytoD (n=64 cells). Note that low CytoD embryos initially constrict before losing adhesion (arrowhead). **(c)** CytoD disrupts contractile pulses. Colorbar represents cross-correlation between constriction rate and the rate of change in Myo-II intensity. Different cells are plotted (Cell index) for different temporal offsets. Note the significant cross-correlation peak around 0 offset in the solvent control. **(d)** Mean cross-correlation between constriction rate and rate in change of Myo-II intensity (p-value <0.0001, using unpaired, two-tailed test for control compared to low or high CytoD at time 0). Data are from representative embryos injected with solvent (n=56 cells), low CytoD (n=86 cells), and high CytoD (n=64 cells). **(e)** CytoD injection causes gaps in the medioapical F-actin meshwork prior to its dissociation from junctions. Image from live Utr::GFP embryo, injected with Low CytoD, demonstrates that F-actin network stretches

prior to cell-cell separation (arrowhead). Image from live Utr::GFP embryo, injected with 0.25mg/mL CytoD (intermediate, Int. CytoD), shows fragmented medioapical F-actin network that is separated from junctions. Scale bars are 5μm.

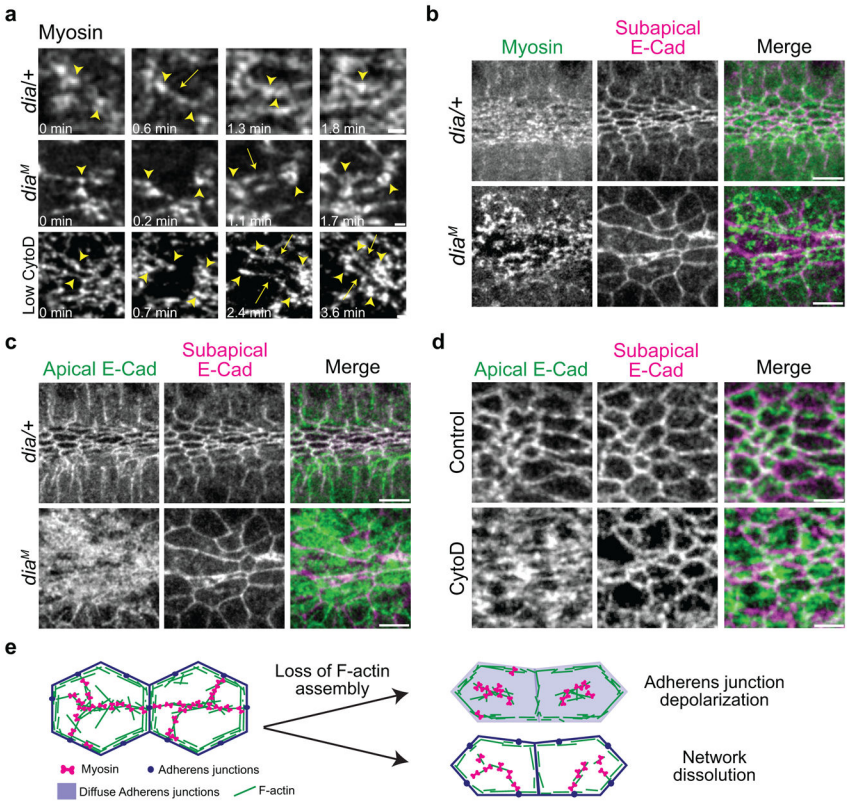

Figure 5.

Dia restricts E-Cadherin to the junctional domain, facilitating contractile network coupling to cell-cell AJs.

(a) Dia is required to couple the medioapical contractile network to junctions. In *dia*^{M} embryos, Myo-II puncta (arrowheads) lose adhesion and separate but can reattach by forming new connections (arrow). Control embryos, *dia/+*, exhibit new connections forming (arrow) and contraction of Myo-II puncta. The *dia*^{M} embryos have similar phenotypes to embryos injected with low CytoD (0.125 mg/mL). Images are apical surface projections from live embryos expressing Myo::GFP. **(b)** In *dia/+* controls, Myo-II forms supracellular meshwork that spans the medioapical surface and across junctions, whereas *dia*^{M} embryos have fragmented medioapical meshworks that fail to maintain connections to junctions. Images are from fixed embryos expressing Myo::GFP (apical surface projection) and stained for E-Cadherin (subapical section). **(c)** Apical E-Cadherin localizes across the apical surface and loses RCP in *dia*^{M} embryos. Images are apical surface projections or subapical section of E-Cadherin from same embryos in **b. (d)** Inhibition of F-actin assembly by CytoD causes accumulation of E-Cadherin across the apical surface, similar to phenotype in *dia*^{M}. Images are from live embryos expressing E-Cad::GFP, injected with solvent (control) or CytoD (0.25 mg/ml). (**e**) Models for loss of contractile network coupling in *dia* mutants. Scale bars are 5μm.

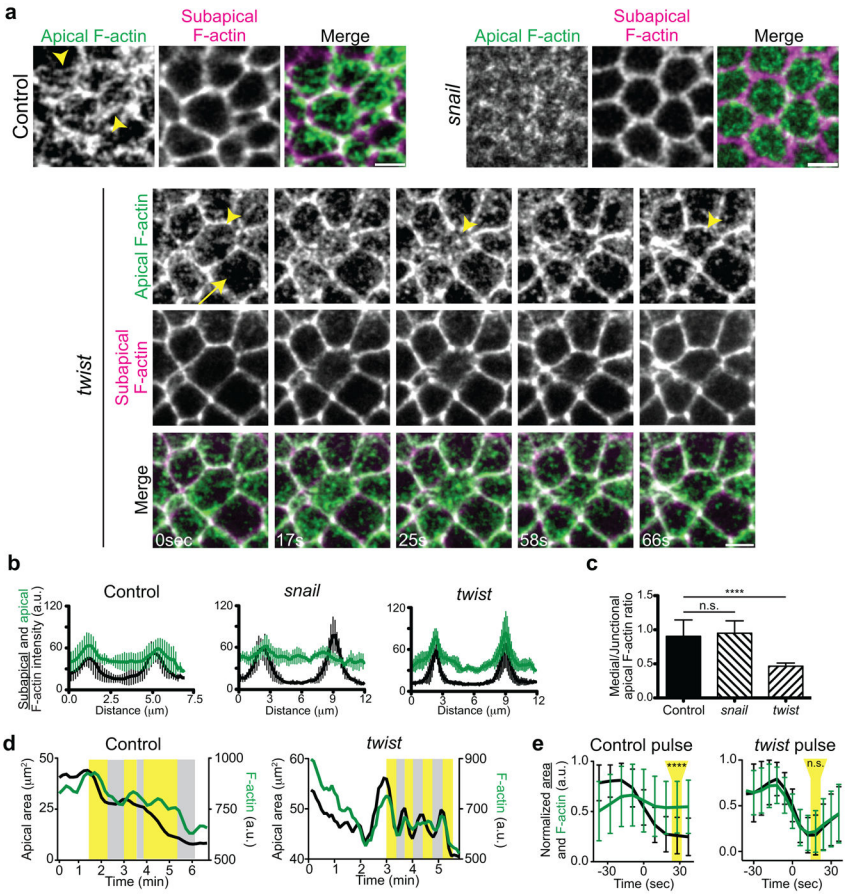

Figure 6.

Twist mediates medioapical F-actin cable assembly.

(a) Twist and Snail are required for medioapical F-actin cable formation. Representative images are from time-lapse movies of control embryos (*twist*/+) and *snail* or *twist* mutants expressing Utr::GFP. Control embryos have more obvious F-actin cables (arrowheads). *snail* mutants have F-actin puncta that fail to form a fibrous meshwork. *twist* mutant constricting cell (arrowhead) has medioapical F-actin condensation during the pulse, but lacks visible F-actin cables before and after pulse. Non-pulsing cells (arrow) have junctional F-actin, but lack medioapical F-actin cables. Scale bars are 5μm. **(b)** Twist is required for the medioapical F-actin meshwork, but not the circumferential F-actin belt. Graphs represent averages of mean fluorescent intensity of apical and subapical F-actin from linescans across cells (n=6) from embryos in **a**. In control cells, F-actin is present in the medioapical cortex and accumulates at junctions. *snail* mutants equally lack both medioapical and junctional F-actin. Error bars are standard deviation. **(c)** *twist* mutants have lower ratio of medioapical:junctional F-actin. Quantifications of average ratio of medioapical to junctional apical F-actin for control (n=25), *snail* (n=25), and *twist* (n=20) cells. Difference between control and *twist* is significant ($p<0.0001$, two-tailed, Mann-Whitney test) but *snail* is not significant (n.s.). Error bars represent standard deviation. Scale bars are 5μm. **(d)** Twist is required to stabilize F-actin levels during contractile pulses. Quantification of apical area and F-actin intensity in individual control and *twist* mutant cell from embryo in **a**. Control

cell contracts (yellow highlight) and F-actin and cell shape is stabilized during contraction. *twist* cells have pulsed contraction (yellow highlight) but do not maintain F-actin stabilization. **(e)** Graphs of average behavior of area and F-actin during contractile pulses from embryos in **a** (above, control n=51 pulses, below, *twist* n=45). Values are normalized to highest and lowest values in individual pulses. Error bars are standard deviation. Yellow highlights indicate time when F-actin levels are significantly increased from apical area in control ($p<0.0001$, two-tailed, Mann-Whitney test) but not in *twist* mutants (n.s.).

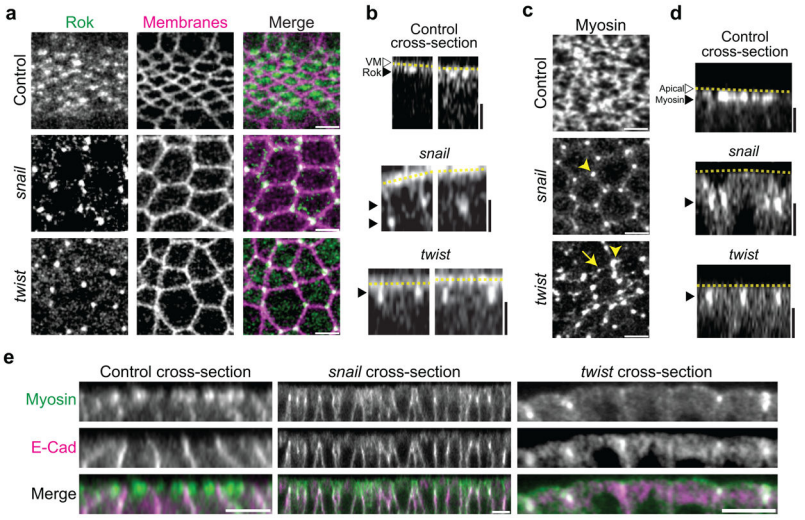

Figure 7.

Twist is required for medioapical radial cell polarity of Rok and Myo-II.

(a) *twist* and *snail* mutants result in an inversion of Rok RCP. Images are apical surface projections from live control, *snail*, or *twist* mutant embryos expressing GFP::Rok(K116A) and Gap43::ChFP. Rok abnormally localizes to junctions at three-way vertices in *snail* and *twist* mutants. **(b)** Rok localizes subapically in *snail* mutants, similar to position of the junctions, while Rok is present apically in control (*twist*/+) or *twist* mutants. Cross-section views of embryos from **a**. Dotted lines indicate the vitelline membrane (VM, white arrowhead). **(c)** Myo-II localization in *snail* and *twist* mutants mirrors Rok localization. Images are from live, control and *snail* or *twist* mutant embryos expressing Myo::GFP. Control embryos (*twist/+)* possess dense medioapical Myo-II meshwork, whereas Myo-II localizes to cell vertices in both *snail* and *twist* mutants (arrowheads). Myo-II transiently appears in medioapical foci in *twist* mutants during constriction pulses (arrow). **(d)** The apical-basal position of Myo-II mirrors the position of Rok. Images are cross-section views of embryos from **c**. Myo-II remains subapical in *snail* mutants, but localizes apically in control and *twist* mutants. **(e)** Apical-basal position of Myo-II corresponds to position of adherens junctions. Myo-II localizes to subapical adherens junctions in *snail* mutants and to apical junctions in *twist* embryos. Images are cross-sections of fixed embryos expressing Myo::GFP and stained for E-Cadherin. Scale bars are 5μm.

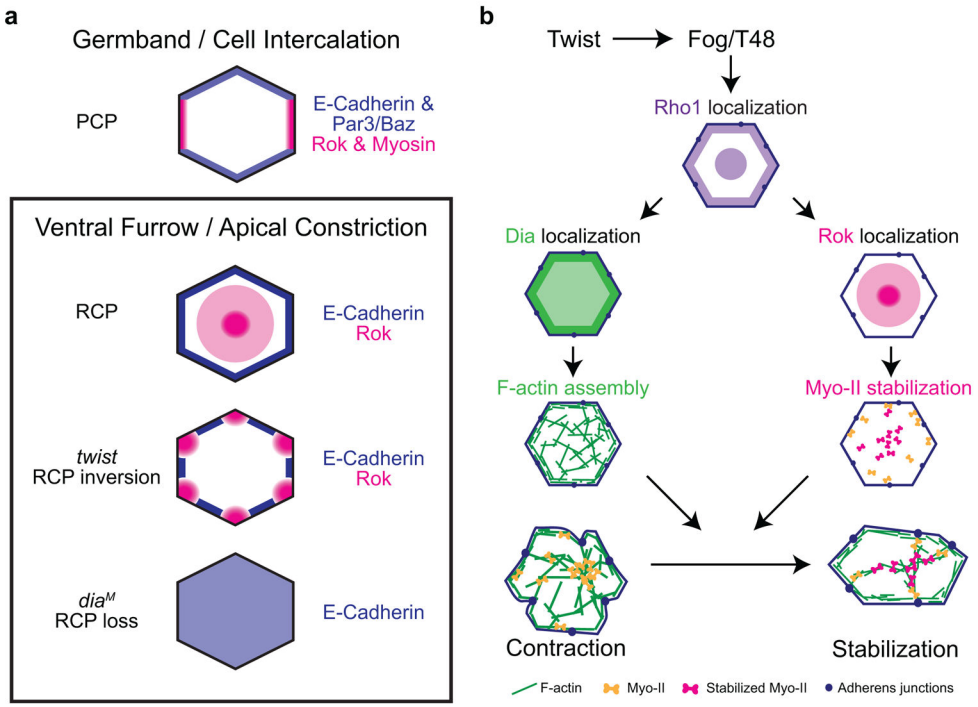

Figure 8.

Radial cell polarity (RCP) coordinates Myo-II stabilization, F-actin assembly, and E-Cadherin localization to facilitate apical constriction.

(**a**) Comparison of cell polarity in germband cells (planar cell polarity, PCP) and ventral furrow cells (radial cell polarity, RCP). Changes in RCP are shown for *twist* and *dia* mutants. Note that we have not analyzed Rok localization in *dia* mutants. (**b**) Model for the Twist-mediated actin-myosin ratchet. Periodic medioapical Myo-II pulses transiently contract the cell (Contraction). Myo-II stabilization and F-actin cable assembly are coordinated to form medioapical contractile fibers that are anchored at AJs and stabilize cell shape fluctuations elicited by pulsing.